

# Linking aptamer-ligand binding and expression platform folding in riboswitches: prospects for mechanistic modeling and design

Fareed Aboul-ela,<sup>1\*</sup> Wei Huang,<sup>2</sup> Maaly Abd Elrahman,<sup>1,3</sup> Vamsi Boyapati<sup>4</sup> and Pan Li<sup>5</sup>

The power of riboswitches in regulation of bacterial metabolism derives from coupling of two characteristics: recognition and folding. Riboswitches contain aptamers, which function as biosensors. Upon detection of the signaling molecule, the riboswitch transduces the signal into a genetic decision. The genetic decision is coupled to refolding of the expression platform, which is distinct from, although overlapping with, the aptamer. Early biophysical studies of riboswitches focused on recognition of the ligand by the aptamer—an important consideration for drug design. A mechanistic understanding of ligand-induced riboswitch RNA folding can further enhance riboswitch ligand design, and inform efforts to tune and engineer riboswitches with novel properties. X-ray structures of aptamer/ligand complexes point to mechanisms through which the ligand brings together distal strand segments to form a P1 helix. Transcriptional riboswitches must detect the ligand and form this P1 helix within the timescale of transcription. Depending on the cell's metabolic state and cellular environmental conditions, the folding and genetic outcome may therefore be affected by kinetics of ligand binding, RNA folding, and transcriptional pausing, among other factors. Although some studies of isolated riboswitch aptamers found homogeneous, prefolded conformations, experimental, and theoretical studies point to functional and structural heterogeneity for nascent transcripts. Recently it has been shown that some riboswitch segments, containing the aptamer and partial expression platforms, can form binding-competent conformers that incorporate an incomplete aptamer secondary structure. Consideration of the free energy landscape for riboswitch RNA folding suggests models for how these conformers may act as transition states—facilitating rapid, ligand-mediated aptamer folding. © 2015 The Authors. *WIREs RNA* published by Wiley Periodicals, Inc.

How to cite this article:

*WIREs RNA* 2015, 6:631–650. doi: 10.1002/wrna.1300

\*Correspondence to: faboulela@zewailcity.edu.eg

<sup>1</sup>Center for X-Ray Determination of the Structure of Matter, University of Science and Technology at Zewail City, Giza, Egypt

<sup>2</sup>Center for Proteomics and Bioinformatics, Case Western Reserve University, Cleveland, OH, USA

<sup>3</sup>Therapeutical Chemistry Department, National Research Center, El Buhouth St., Dokki, Cairo, Egypt

<sup>4</sup>Department of Biochemistry and Molecular Biology, Louisiana State University Health Sciences Center, New Orleans, LA, USA

<sup>5</sup>Department of Biological Sciences, University at Albany—SUNY, Albany, NY, USA

Conflict of interest: The authors have declared no conflicts of interest for this article.

## INTRODUCTION

Riboswitches are natural, 'smart' nanodevices. They are RNA molecules that combine biosensing with real-time genetic decision making. The biosensing portion of the riboswitch is called the aptamer. To couple the aptamer sensing event to gene expression, the riboswitch must have the capacity to alter its folding pathway in response to a ligand-binding signal. This review asks how the binding of a ligand to the aptamer perturbs the RNA folding trajectory?

Artificial aptamers were developed for numerous applications before natural aptamers were discovered within riboswitches.<sup>1</sup> The coupling of the aptamer/biosensor with a gene expression switch opens new applications, most immediately in synthetic biology.<sup>2–4</sup> As riboswitches have been observed primarily in bacteria, they also attract attention as a target for the design of novel antibiotics.<sup>5–7</sup> A better mechanistic understanding of riboswitch function could enhance both types of applications.

We consider how the ligand-binding event is transduced into a gene expression signal. To address this question, it is necessary to consider the communication between biosensing (aptamer) and regulatory (expression) domains. We focus on transcriptional riboswitches, which compel us to transcend the classic structural biology approach, and consider a number of dynamic factors, specifically: (1) The system is intrinsically prone to conformational heterogeneity.<sup>8–10</sup> (2) The free energy landscape (FEL) that defines the relative stability of conformers is continually changing as the transcription proceeds.<sup>11–15</sup> (3) Kinetic factors may therefore control the outcome, but a number of rates need to be considered, including but not limited to ligand binding, RNA (re)folding, and movement and pausing of the polymerase and the transcription complex. (4) All of these rates are highly sensitive to cellular conditions. The riboswitch can therefore be tuned to respond to the cellular environment in a complex way.<sup>10,16,17</sup> (5) When considering the coupling between ligand binding and RNA folding, it is important to consider binding-competent conformers that do not form the full aptamer,<sup>17–20</sup> as ligand interactions with these conformers can have a profound effect on the RNA folding pathway. In this review, we re-evaluate earlier work, including X-ray structures of isolated aptamer/ligand complexes, biophysical studies, modeling, and simulations. Our focus is what mechanism(s), in light of the dynamic considerations listed above, might transduce the ligand-binding signal into the genetic decision.

## THE P1 HELIX PLAYS A KEY MECHANISTIC ROLE IN MANY RIBOSWITCHES

Riboswitches can be classified according to a number of criteria: effector ligand,<sup>21</sup> Rfam folding family,<sup>22</sup> mode of regulation (e.g., transcription vs translation),<sup>23</sup> complexity of organization,<sup>24</sup> or aptamer structural<sup>10,25</sup> and binding properties.<sup>24</sup> The early exploration of coupling between ligand binding and expression platform folding highlights variations in riboswitch function within families,<sup>26</sup> or even for an

individual riboswitch,<sup>16,17</sup> depending on conditions. These distinctions are arguably as significant as those between the behavior of individual riboswitch families or superfamilies. In this review, we start by considering common aspects of the coupling/switching mechanism for a set of riboswitches which we call ‘P1 helix-regulated riboswitches’.

Many of the most intensely studied riboswitches, including purine, thiamine pyrophosphate (TPP), *S*-adenosyl methionine (SAM), lysine, and flavin mononucleotide (FMN) riboswitches, fall into the P1 helix-regulated category. These were also some of the first riboswitches discovered. For these reasons, this set forms the focus of this review. Although most riboswitches are divided into those which operate by transcriptional or translational attenuation, we focus on transcriptional riboswitches. We will not further consider systems that combine the riboswitch mechanism with splicing, cleavage, sequestration of protein<sup>27</sup> or silencing.<sup>28</sup>

More complex riboswitches, such as the Mg<sup>2+</sup>,<sup>29</sup> glycine<sup>30</sup> and *c*-di-AMP riboswitches,<sup>31</sup> which contain tandem or multiple ligand-binding sites, or the B12 riboswitch,<sup>32</sup> are likely to present novel and more complex mechanistic features. At the other end of the spectrum, the pre-queuosine and SAM-II riboswitches could arguably be described as special cases of P1 helix-regulated riboswitches with a single helix within the aptamer domain. As we will see (next section), the formation of the P1 helix from nonadjacent sequences is central to the explanation of the conformational coupling phenomenon in P1 helix-regulated riboswitches. We will not further consider the pre-Q riboswitches, which have been reviewed elsewhere.<sup>33</sup>

## P1 Helix-Regulated Riboswitches

We define a P1 helix-regulated riboswitch by the following characteristics (Figure 1(a)): (1) A series of two or more stem loops form within the aptamer domain via base pairing of *adjacent* strand segments. (2) *Nonadjacent* segments on either side of the aptamer domain come together to form the P1 helix in the presence of the ligand. This helix is the only long range, or at least the longest range, pairing interaction required by the secondary structure. (3) The stabilization of the P1 helix results in the formation of an  $n > 2$  helix junction that forms the core of the aptamer. (4) The P1 helix is often metastable. If the P1 helix fails to form, the nonligand binding riboswitch structure may be described as a series of stem loops formed from adjacent strand segments extending into the expression domain. (5) The 3' strand of the P1 helix overlaps between aptamer and expression domains. It can also

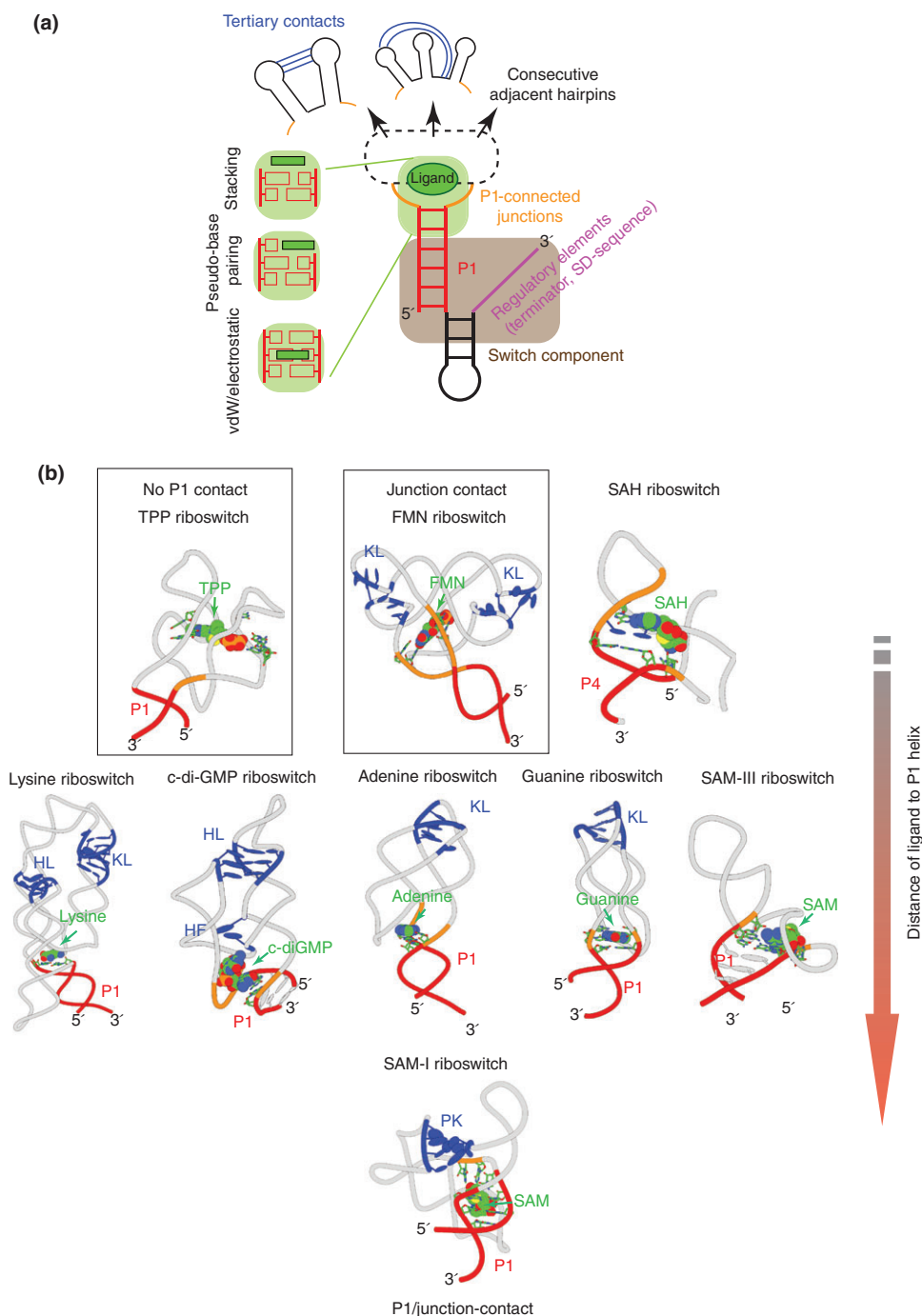


**FIGURE 1** | Riboswitch ligands bring P1 helix strands together. (a) Schematic of P1 helix riboswitch showing three domains of the aptamer and overlapping expression domain. (b) Position of ligand above P1 helices within structures of ligand/aptamer complexes from P1 helix-regulated riboswitches. The backbone of the riboswitch is shown as tube with the P1 helix highlighted in red, and junctions connecting P1 strands are in orange. The ligand is shown as sphere, and nucleotides that have contacts with the ligand in either the P1 helix or junctions connecting P1 strands are shown as stick. Tertiary structural motifs, such as pseudoknot (PK), kissing loop (KL), helix-loop (HL) contacts, and nonadjacent nucleotide stack ('high-five' stack, HF) are highlighted in blue. Protein databank (PDB) entries used in this figure are: TPP riboswitch (2cky), FMN riboswitch (3f2q), S-adenosyl homocysteine (SAH) riboswitch (3npq), Lysine riboswitch (3dil), c-di-guanine mononucleotide phosphate (GMP) riboswitch (3irw), Adenine riboswitch (1y26), Guanine riboswitch (1y27), SAM-III riboswitch (3e5c), and SAM-I riboswitch (2gis). These riboswitches are classified into three types based on the relative position of ligand to the P1 helix. For the largest group, the ligand clearly stabilizes the closing base pair of the P1 helix through direct contact (middle and lower panels), or indirectly via contacts with linking strands (FMN riboswitch). In one case (SAH), the P4 helix plays the functional role of P1 and shows a similar pattern of contacts with the ligand. Only TPP lacks obvious stabilizing contacts with the P1 helix.

form an alternate pairing with a downstream segment. This pairing blocks formation of a downstream terminator (in a positively regulated transcriptional riboswitch) or antiterminator helix (in a negatively regulated transcriptional riboswitch) or competes for hybridization with a Shine–Dalgarno (SD) or anti-SD segment (translational riboswitch).

### Three-Dimensional Architecture of P1 Helix-Regulated Riboswitch Aptamers

Inspection of high-resolution three-dimensional (3D) structures of many riboswitch aptamers (Figure 1) confirms that they can be analyzed as a set of three domains. A set of stem loops link together with the P1 helix via the junction. A single nonadjacent P1 helix pairs opposite ends of the aptamer. The genetic purpose of this device is to bring the nonadjacent segments of the P1 helix together or keep it apart, in response to the ligand signal, thus determining a signaling outcome downstream (Figure 1(a)).

In addition, riboswitch aptamers of this category contain long-range tertiary interactions such as loop–loop (lysine<sup>16</sup> and some purine riboswitches<sup>24</sup>) and pseudoknot (SAM-I) interactions.<sup>34,35</sup> These tertiary interactions are coupled to the presence of structural motifs such as base triples and quadruples,<sup>24</sup> A-minor interactions and kink turns<sup>36</sup> (Figure 1(b)). The motifs and tertiary interactions may be stabilized by ligand binding,<sup>36</sup> and are also sensitive to cellular conditions, notably magnesium levels.<sup>34,37</sup> This aptamer organization is ideally tuned to (1) detect the metabolic state of the cell and (2) transduce the information to the downstream secondary structure folding via P1 helix stabilization or destabilization.

The task of the ligand, therefore, is to enhance P1 helix formation at the expense of competing pairings with downstream segments. This task is closely coupled to the overall 3D arrangement of the set of stem loops. As pairing of the P1 helix severely restricts the sampling of 3D arrangements for the multiple stems and junction, it incurs an entropic penalty. Furthermore, P1 helix formation is likely to be the rate-limiting step in aptamer folding, and possibly in ligand binding, at least when the ligand concentration is well above the  $K_d$ .

Ligand-aptamer contacts observed in most X-ray structures of P1 helix-regulated riboswitch aptamers (Figure 2) are consistent with ligand stabilization of the P1 helix.<sup>24,38</sup> In most aptamer–ligand complexes, the ligand sits directly above or near the closing base pairs of the P1 helix, often making nonbonded interactions (Table 1, Figure 1(b)). In some cases (SAM-I,<sup>39,40</sup> SAM-II<sup>41</sup>), the ligand directly contacts these closing base pairs (Figure 1(b)). In these cases, and in the cases

of adenine, guanine, SAM-III,<sup>42</sup> lysine, and c-di-GMP riboswitches,<sup>43</sup> the ligand contains a ring that stacks near a residue in the closing base pairs of the P1 helix, providing further stabilization (Figure 1(b), middle panel). Finally, important contacts, including hydrogen bonds (Table 1, Figure 2) are observed between the ligands and junctions that link the P1 helix to adjacent helices. Ligand–junction contacts stabilize P1 formation by countering the entropic penalty for restricting the arrangement of junction strands. Only in the TPP riboswitch,<sup>44,45</sup> does the ligand make no direct contacts either with the P1 helix or adjacent junctions.

In Figure 1(b), upper panel illustrates two exceptional cases in addition to the TPP riboswitch aptamer. In the FMN riboswitch aptamer, FMN makes no P1 helix contacts but there are important contacts with both junctions linking to the P1 helix. These contacts restrict the conformational flexibility of P1-linked junction segments, facilitating P1 helix formation as achieved in a more direct form for other riboswitches. The S-adenosyl homocysteine (SAH) riboswitch is a special case in that the P4 helix is formed from nonadjacent strands and plays the strand-exchanging role associated with P1 helices in other riboswitch aptamers. The ligand stacks with the closing base pair of the P4 helix, and contacts the adjacent junctions (Figure 1(b), lower panel), as observed for the P1 helix in other riboswitch aptamers, consistent with the interpretation that the ligand stacking in both cases is important for stabilizing nonadjacent helices.

When contacts are observed to two helices, or to two junction strands, such mutual contacts constrain the distances and relative orientations of the respective architectural elements within the riboswitch fold. Figure 2 shows the corresponding constrained distances as measured from X-ray coordinates of several ligand/riboswitch aptamer complexes. Some ligands contact negatively charged phosphate backbones on junction strands linked to opposing strands of the P1 helix. Some of these contacts are Mg<sup>2+</sup> mediated.

### Riboswitch Aptamers Hint at a Much More Dynamic Picture

A deficiency of an analysis based upon X-ray coordinates is that biological processes are dynamic. Specifically, transcription is a stochastic process resembling a biased random walk. Nonetheless, the pattern of ligand contacts to P1 helices in the 3D structures of riboswitch aptamers (Table 1, Figure 2), even with the expression domains truncated, hints at the dynamic tendency of riboswitches to form alternate helices. The role of contacts observed in X-ray coordinates in P1 helix stabilization can be tested in simulations, as well as

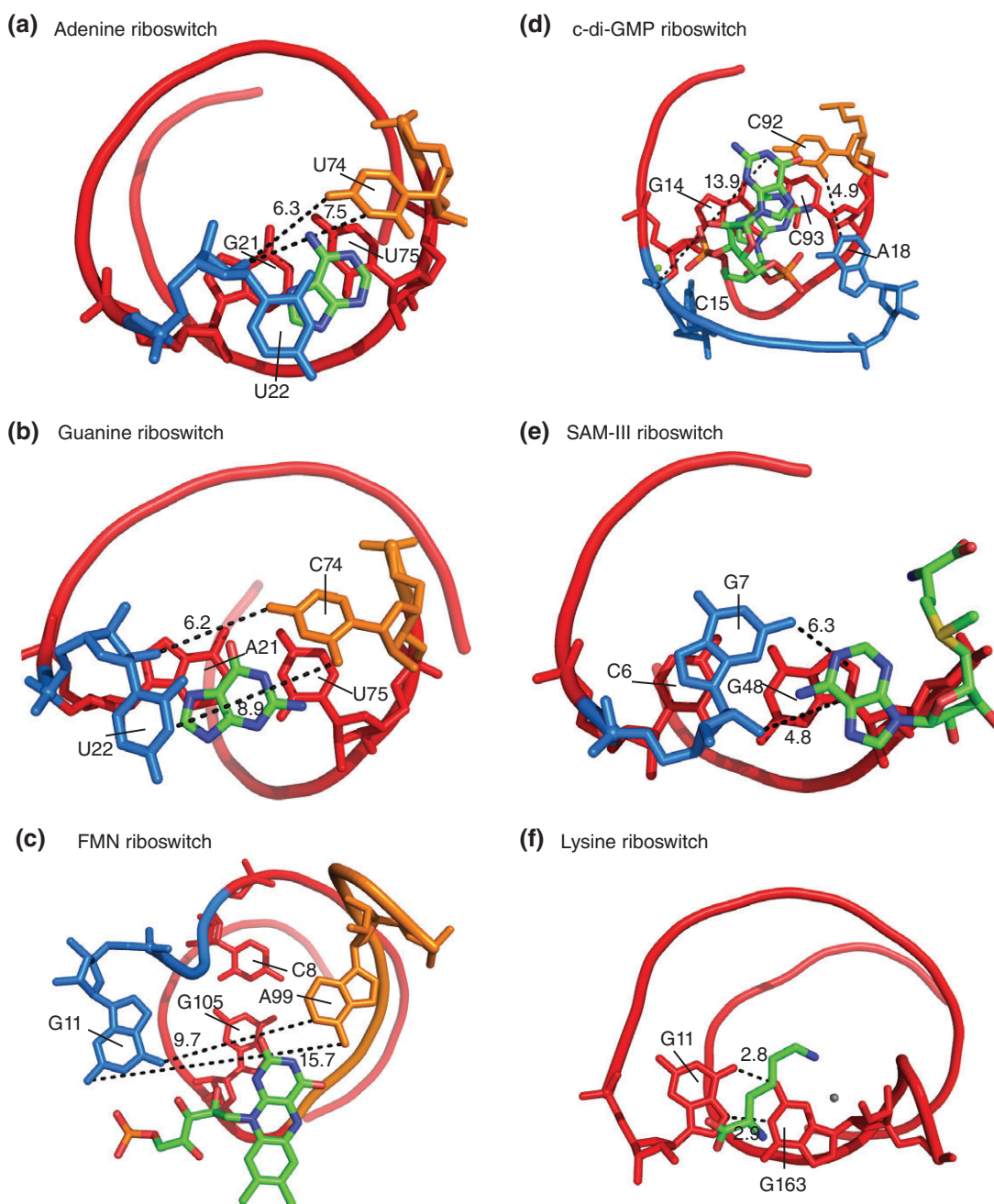


**FIGURE 2** | Ligand contacts constrain the placement of P1 helix-forming strands, favoring helix formation. Distances between P1 helix strands or their flanking junctions upon ligand binding in angstroms are highlighted. Maximum and minimum distances between atoms on the distal P1 helix-forming strand segments (or adjacent ‘junction’ segments) that contact the ligand, either directly or via water molecule or magnesium ion, are indicated as dashed lines. As ligand binding constrains the distances between nonadjacent strands, it facilitates strand association and P1 helix formation. In panels a–f, the ligand is colored by element, red sticks are the closing base pair of P1 helix, blue sticks/ ribbon are J1/2, orange sticks/ ribbon are J3/1 (but J6/1 in FMN riboswitch), red ribbons are P1 helix strands, gray sphere is a water molecule, and green sphere is a magnesium ion. (a) Adenine riboswitch, (b) Guanine riboswitch, (c) FMN riboswitch, (d) c-di-GMP riboswitch, (e) SAM III riboswitch, and (f) Lysine riboswitch.

experimentally using mutational analysis, and fluorescence and other biophysical monitors of riboswitch folding and ligand binding.

The Sanbonmatsu group<sup>46</sup> modeled SAM-induced folding atomistically in the *Thermoanaerobacter*

*tengcongensis* SAM-I riboswitch using structure-based simulation with explicit solvent. Native contacts between SAM and the aptamer, as observed in an X-ray structure of the complex, were incorporated as attractive interactions. P1 formation appeared as the

**TABLE 1** | List of Ligand Contacts with Riboswitch Aptamers Based upon X-Ray Coordinates (List of PDB Id Codes)

Riboswitch	Segment	Residues	Type of Interaction	Note	
Lysine riboswitch (3dil)	P1	<b>G11•G163</b>	<b>Nonbonded interaction, hydrogen bond, and mediated hydrogen bond</b>	<ul style="list-style-type: none"> <li>• Closing base pair of P1</li> <li>• G163 via a water bridge</li> <li>• G11 via hydrogen bond and a coordinated potassium cation</li> </ul>	
	P2	G12	Hydrogen bond and mediated hydrogen bond	<ul style="list-style-type: none"> <li>• Via coordinated potassium cation</li> <li>• Forms the closing base pair with C79</li> </ul>	
	P2	G14	Mediated hydrogen bond	<ul style="list-style-type: none"> <li>• Via coordinated potassium cation</li> </ul>	
	P4	G114	Hydrogen bond	<ul style="list-style-type: none"> <li>• Via water bridge and a direct hydrogen bond</li> </ul>	
	P4	G115	Mediated hydrogen bond	<ul style="list-style-type: none"> <li>• Forms the closing base pair with U140</li> </ul>	
	J2/B	G80	Hydrogen bond	<ul style="list-style-type: none"> <li>• Via coordinated potassium cation</li> </ul>	
	J2/B	A81	Nonbonding interaction	<ul style="list-style-type: none"> <li>• Sandwiched between ligand and closing P1 base pair</li> </ul>	
	c-di-GMP riboswitch (3inw)	P1	<b>G14-C93</b>	<b>Stacking</b>	<ul style="list-style-type: none"> <li>• Closing base pair of P1</li> </ul>
		J1/2	C15	<b>Mediated hydrogen bond</b>	<ul style="list-style-type: none"> <li>• Via coordinated magnesium cation</li> </ul>
		J1/2	C17, A18, G19, G20	<b>Hydrogen bond</b>	<ul style="list-style-type: none"> <li>• G20 forms pseudo base pair with ligand</li> </ul>
J3/1		C92	<b>Hydrogen bond</b>	<ul style="list-style-type: none"> <li>• Forms pseudo base pair with ligand</li> </ul>	
P2		G21-C46	Stacking	<ul style="list-style-type: none"> <li>• Closing base pair</li> </ul>	
J2/B		A47	Stacking	<ul style="list-style-type: none"> <li>• Sandwiched between ligand guanine moieties</li> </ul>	
J6/1		A99	<b>Hydrogen bond</b>	<ul style="list-style-type: none"> <li>• Forms pseudo base pair with ligand</li> </ul>	
J1/2		<b>G10, G11</b>	<b>Hydrogen bond</b>	<ul style="list-style-type: none"> <li>• Recognize the phosphate group of ligand</li> </ul>	
J2/B		G32	Hydrogen bond		
J4/5		G62	Hydrogen bond		
FMN riboswitch (3f2q)	J2/B	G33	Mediated hydrogen bond	<ul style="list-style-type: none"> <li>• Via coordinated magnesium cation</li> </ul>	

**TABLE 1** | Continued

Riboswitch	Segment	Residues	Type of Interaction	Note
SAM-III riboswitch (3e5c)	J5/6	G84	Hydrogen bond	<ul style="list-style-type: none"> <li>• These two residues sandwich the ligand</li> </ul>
	J5/6	A85	Stacking	
	J3/4	A48	Stacking	
	<b>P1</b>	<b>G48</b>	<b>Stacking</b>	<ul style="list-style-type: none"> <li>• <b>Forms the closing base pair with C6</b></li> <li>• <b>Forms pseudo base pair with ligand</b></li> </ul>
	<b>J1/2</b>	<b>G7</b>	<b>Hydrogen bond</b>	
	J2/4	U37	Stacking	<ul style="list-style-type: none"> <li>• Via a water bridge</li> <li>• <b>Closing base pair of P1</b></li> <li>• <b>Forms pseudo base pair with ligand</b></li> </ul>
	J2/4	A38	Hydrogen bond	
	J2/4	A39	Hydrogen bond	
	<b>P1</b>	<b>A21-U75</b>	<b>Stacking</b>	
	Guanine/adenine riboswitch (1y27/1y26)	<b>J3/1</b>	<b>C/U74</b>	<b>Hydrogen bond</b>
<b>J1/2</b>		<b>U22</b>	<b>Stacking</b>	
J2/3		U47	Hydrogen bond	
J2/3		U51	Hydrogen bond	
J2/3		A52	Stacking	
SAH riboswitch (3NPQ)	<b>J1/4</b>	<b>G47</b>	<b>Hydrogen bond</b>	<ul style="list-style-type: none"> <li>• <b>Forms pseudo base pair with ligand</b></li> </ul>
	<b>J4/2</b>	<b>G15</b>	<b>Hydrogen bond</b>	
P4-controlled riboswitch	J2/1	A29	Stacking	<ul style="list-style-type: none"> <li>• <b>Forms pseudo base pair with ligand</b></li> </ul>
	J2/1	G30, G31	Hydrogen bond	

Contacts with P1 helices and junction segments linked directly to the P1 helix-forming strands will restrict the relative orientations of these strand segments, significantly reducing the entropic penalty for juxtaposing P1 strand segments. Such contacts are highlighted in bold, as are the contacts to junctions linking to P4 in the SAH riboswitch.

SAH, S-adenosyl homocysteine.

final step in folding, but occurred faster in the presence than in the absence of SAM. Direct molecular dynamics (MD) simulations on the same riboswitch highlighted the role of direct contacts between SAM and the G11 residue in the junction (J12) linking the P1 and P2 helices.<sup>47</sup> Additional  $Mg^{+2}$  mediated interactions between SAM and other junction residues were remarkably stable during long-timescale MD runs.<sup>19</sup> Structure probing through susceptibility to chemical modification and interference confirmed that tertiary folding characteristic of the ligand-bound aptamer is linked synergistically to both SAM and  $Mg^{+2}$  concentrations.<sup>37</sup>

Additional P1 helix stabilization via direct contacts with SAM in the X-ray structure explains increases in  $K_d$  for SAM binding for aptamers containing mutations in two P1 helix base pairs near the junction-observed by isothermal titration calorimetry (ITC)<sup>48</sup> and equilibrium dialysis.<sup>49</sup> Further evidence for a link between SAM binding and P1 helix formation in this riboswitch comes from a correlation between P1 helix length and ligand binding as measured by fluorescence resonance energy transfer (FRET).<sup>50</sup> Single-molecule fluorescence measurements in the SAM-I riboswitch indicate that ligand binding is coupled to a rotation in P1 helix orientation relative to the core/junction riboswitch region.<sup>50</sup> This finding may be interpreted in the context of the ligand positioning aptamer subdomains in a manner that facilitates coaxial stacking between individual helices, a common feature of folded branched nucleic acid structures.

MD simulations of the Adenine riboswitch also highlighted contacts with a junction region stabilizing a 3D configuration favorable for P1 helix formation.<sup>51</sup> For the purine riboswitches, loop-loop interactions involving helices P2 and P3 have been linked to P1 stability using mutational analysis, FRET and time-resolved nuclear magnetic resonance (NMR) (reviewed in Ref 9). A particularly interesting case is the *pubE* adenine riboswitch. Single-molecule pulling studies indicated that P1 helix formation was metastable at least in the absence of ligand<sup>52</sup> even for the truncated aptamer.

## DYNAMIC ASPECTS OF RIBOSWITCH FUNCTION

### Cotranscriptional Folding and Function of Riboswitches

When riboswitches are regulating transcription or translation in the cell, many factors interact, including the DNA and RNA, the polymerase and accompanying factors, as well as the effector ligand and possibly cellular proteins, such as *Nus*.<sup>53</sup> Timing and coordination between the binding and association of these factors,

the movement of the transcription complex, and the RNA folding are critical to the outcome. It cannot be assumed that individual steps, including riboswitch folding and ligand association, will reach equilibrium before the genetic decision takes place. A recent study of *Escherichia coli* coenzyme B12 binding *btuB* riboswitch folding and function using a pausing-deficient  $\beta'$ F773V RNA polymerase revealed a profound effect on regulatory outcome.<sup>54</sup> The interplay with cotranscriptional folding and ligand binding is further complicated by heterogeneity amongst populations of RNA polymerase molecules.<sup>55</sup>

Conformational dynamics, stochasticity, non-equilibrium processes, and heterogeneity must therefore be incorporated into any analysis of riboswitch function in transcription.

### The Role of Ligand Binding Kinetics in Kinetic Control

A seminal series of early papers measured binding kinetics for transcriptional riboswitches with cognate FMN and purine ligands.<sup>14,15</sup> The predicted equilibration time for ligand binding was shown to be comparable to or slower than the timescale for transcription of the riboswitch, at least under certain conditions. Translational riboswitches, on the other hand, may be able to reach a folding and binding equilibrium before the ribosome has a chance to recognize the SD sequence.

These findings addressed an apparent discrepancy in early riboswitch data between the apparent  $K_d$  for ligand binding, and the threshold concentration of ligand required for 50% activation/suppression of gene expression, as measured *in vitro* or *in vivo*.<sup>8</sup> The kinetic data offered an explanation: ligand levels must be high enough to stabilize the aptamer complex during the timescale of transcription, which should be higher than that required at equilibrium.

A 2012 study on the lysine riboswitch provided direct evidence of both thermodynamic and kinetic control, depending on the nucleotide levels in an *in vitro* transcription assay.<sup>16</sup> When transcriptions were performed at 50  $\mu$ M NTP concentrations using a DNA template coding for the wild-type *Bacillus subtilis* *lysC* gene and leader sequence, a correlation was observed between  $T_{50}$  (the concentration at which transcription is 50% terminated) and  $K_d$  for lysine and a series of riboswitch-binding analogs. This correlation, though, did not hold up at higher nucleotide concentrations.

The lysine riboswitch study is arguably the exception that proves the rule, that at least in general, transcriptional riboswitches are kinetically controlled. On the other hand, the low NTP concentration conditions



that give rise to thermodynamic control in the *in vitro* experiments are relevant to stationary phase conditions. The capacity to switch between kinetic and thermodynamic control may allow the cell to adjust the threshold ligand concentration for suppression of gene expression when appropriate.

## The Role of RNA Folding Kinetics in Kinetic Control

Kinetic control is often described by assuming that the genetic decision is made at the time that the aptamer is transcribed<sup>14,15,24</sup> (Figure 3). In this scenario, ligand binding fixes the aptamer fold before the expression platform is synthesized. In the absence of the ligand, the aptamer, if it forms, is relatively unstable and will not compete effectively with formation of competing downstream helices once the latter have been transcribed. The model assumes that aptamer folding can take place before the expression platform is transcribed, at least if the ligand is present. If so, then ligand-binding properties for the aptamer, whether thermodynamic or kinetic, should determine the outcome.

On the other hand, early kinetic studies detected a second-order exponential decay in fluorescence binding curves.<sup>14</sup> Moreover, the authors pointed out that the observed dynamic range in gene expression never represented more than 50% of transcription complexes, which they interpreted as indicating that many riboswitches form ‘off-pathway’ species.<sup>14</sup> Such variation is characteristic of many levels of cellular regulation and similar observations for other riboswitches lead to the term ‘dimmer switch’ for riboswitch gene regulation.<sup>56</sup> Thus, in addition to kinetics of ligand binding, kinetics of riboswitch folding must be considered. Computationally, it is feasible to model a number of scenarios varying relative rates for binding, folding, transcription, pausing, and transcript stability<sup>37</sup> in which any combination of these processes may be rate limiting.

Relatively few riboswitch folding kinetic studies have appeared.<sup>58,59</sup> Most of them focus on the aptamer segment, although the expression domain was included in some kinetic studies of ligand binding.<sup>14,15,60–63</sup> Aptamer folding is temperature dependent and may take place on the timescale of transcription near 37°C. Folding and binding rates depend on ambient conditions and the riboswitch sequence itself, and the cells’ metabolic state. Moreover, transcription rates, including sites and lengths of pauses,<sup>54,55</sup> vary depending on cellular conditions. While a general consensus has emerged that transcriptional riboswitches are often kinetically controlled, caution has rightly been exercised in generalizing this conclusion.

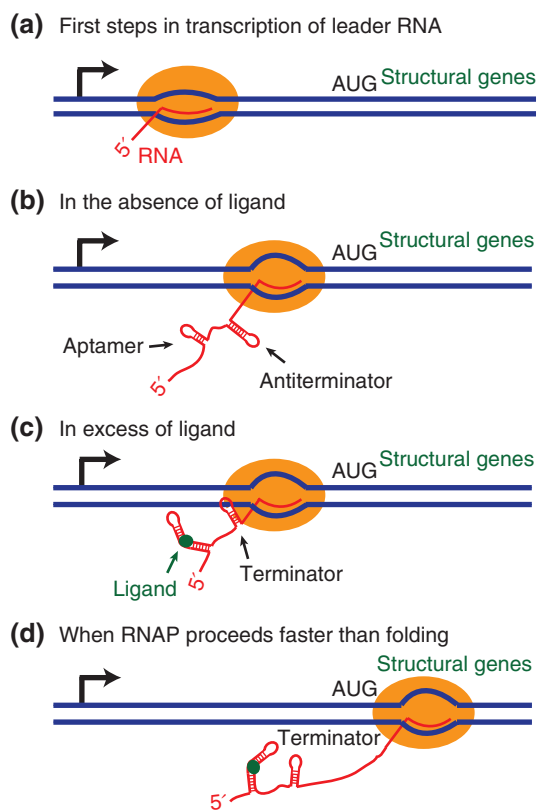


**FIGURE 3** | Schematic illustration of classical kinetic trapping model for ligand-induced riboswitch aptamer folding under kinetic control. Transcription is initiated (panel a) upstream of the start site (AUG). In the absence of ligand (b) the nascent transcript forms a series of hairpin loops from adjacent strand segments, including a secondary structure element in the expression platform. This element may be an antiterminator (for a negatively regulated transcriptional riboswitch, as shown) or a terminator (positively regulated transcriptional riboswitch) or it may sequester or expose an SD sequence (positively or negatively regulated translational riboswitch), respectively. This model assumes that the distal strand segments constituting the P1 helix can anneal before segments involved in competing downstream helices are fully transcribed. If there is sufficient ligand to bind to and fix aptamer folding (c) before the completion of expression platform transcription then aptamer formation prevents antiterminator formation, which in turn enables terminator formation further downstream. If the transcription complex reaches the start site before the terminator folds (d) transcription could proceed in the presence of the ligand.

## LIGAND BINDING AND RIBOSWITCH FOLDING PATHWAYS

### Simulating Cotranscriptional Folding Using the FEL

Whether the riboswitch mechanism operates by kinetic or thermodynamic control, the question remains as to how the ligand perturbs the conformational distribution. If the mechanism is kinetic, the question becomes

more complex, because the presence of the ligand may affect the rate of folding, as well as the thermodynamic stability of competing structures. This kinetic factor compels us to consider folding pathways and intermediate or transition state folds. We must then recall that RNA, even under equilibrium conditions, is not restricted to two states, but forms a population distribution as determined by the FEL.<sup>64,65</sup>

It is important to recognize that the FEL is not a descriptive model. It is solidly based in the statistical mechanics principles that govern folding and interactions of biomolecules in solution. If the experimental parameters to calculate the FEL are available, statistical mechanics and transition state theory can be used to make quantitative predictions.

A starting point for the analysis of cotranscriptional folding is to simulate transcriptional elongation by computing predicted populations of conformers for riboswitches as a function of transcript length.<sup>11–13</sup> We computed base pair probabilities (BPPs) for varying length SAM-I riboswitch transcripts, starting with the complete aptamer and extending to transcripts containing the full expression platform, including potential terminator and antiterminator hairpin-forming sequences. Although SAM-I riboswitches from different sources show variations in predicted behavior, the dominant pattern was aptamer formation for the shortest and the longest transcripts. Antiterminator forming structures appear only during a ‘sensing window’,<sup>11</sup> near completion of antiterminator synthesis. For a series of riboswitches Quarta et al.<sup>11,12</sup> concluded that an early occurrence of the sensing window, following the transcription of the full aptamer domain, is correlated with kinetic control. The predictions imply that it is the binding-incompetent structure that is trapped kinetically in the absence of ligand, and that transcription must proceed past the aptamer before the RNA folding decision is reached.

The same studies also provided insight into the nature of the unliganded riboswitch conformational states. Predicted alternative folds in the TPP riboswitch<sup>11</sup> in the sensing window provided an explanation for the failure of TPP riboswitches of intermediate length to bind the ligand—as assayed via quenching of 2-aminopurine fluorescence due to P1 helix formation.<sup>62</sup> Similarly, an alternative fold for the unliganded SAM-I riboswitch, involving sequestration of one P1 helix segment by a P4 helix segment was predicted.<sup>13</sup> The prediction is validated retrospectively from early in-line probing data<sup>49</sup> by comparison with new data for constructs in which the 5′ P1 segment was truncated<sup>18</sup> (Figure 4). Interestingly, the alternative conformation is formed completely from segments that are transcribed before aptamer synthesis has been completed.

## The Competition between P1 and Alternative Helix Formation: A Role for Strand Migration?

While conformational population distributions can be described by a Boltzmann factor at equilibrium, they may deviate significantly during the cotranscriptional folding process, depending on kinetics of folding. FEL-based calculations such as those described above may allow us to link the population distributions to the kinetics of folding, with caveats. Specifically, if we can hypothesize as to the most favorable folding pathways between two or more free energy minima, we can estimate rates based on the energetic barriers between intermediate ‘transition’ states along these pathways.<sup>66,67</sup>

Overall, computational studies, atomistic as well as thermodynamic and kinetic, predict that P1 helix formation is the rate-limiting step in cotranscriptional aptamer folding for some purine and SAM riboswitches.<sup>13,46,51,68,69</sup> Single-molecule folding studies have confirmed this expectation for the TPP and pubE adenine riboswitches.<sup>52,70</sup> Additional evidence comes from NMR studies.<sup>58,71</sup> Kinetics of and pathways for P1 helix formation should therefore be a major focus of the cotranscriptional folding analysis.

During the sensing window, small populations of what we termed ‘hybrid structures’ containing partially formed P1 helices and partially formed antiterminator helices are predicted.<sup>13</sup> Analog *B. subtilis yitJ* SAM-I riboswitches that were constrained to form the hybrid folds bind to SAM in the micromolar  $K_d$  range, two to three orders of magnitude weaker than for the truncated aptamer.<sup>18</sup>

Previously, it had been assumed that antiterminator formation would be irreversible during cotranscriptional folding. For the same SAM-I system, fluorescence-based assays indicated that SAM binding could not fully reverse the formation of bimolecular analogs of the antiterminator containing conformers.<sup>13,63</sup> The unimolecular system will be a different case, however. A 3-microsecond unconstrained MD simulation of the same system, using the special computing facility Anton, captured a branch migration event in the presence of SAM converting antiterminator helix base pairs to P1 helix base pairs.<sup>19</sup> Single-molecule force studies indicate folding transitions on a similar timescale for analogous molecules,<sup>72</sup> indicating the plausibility of the event observed in the simulation. Theoretical calculations propose this branch migration as the fastest route toward strand switching.<sup>73</sup>

Taken together, the experimental studies and simulations cited in this section indicate that a SAM-I riboswitch with a partly formed antiterminator can be rapidly converted to a full P1 helix-forming

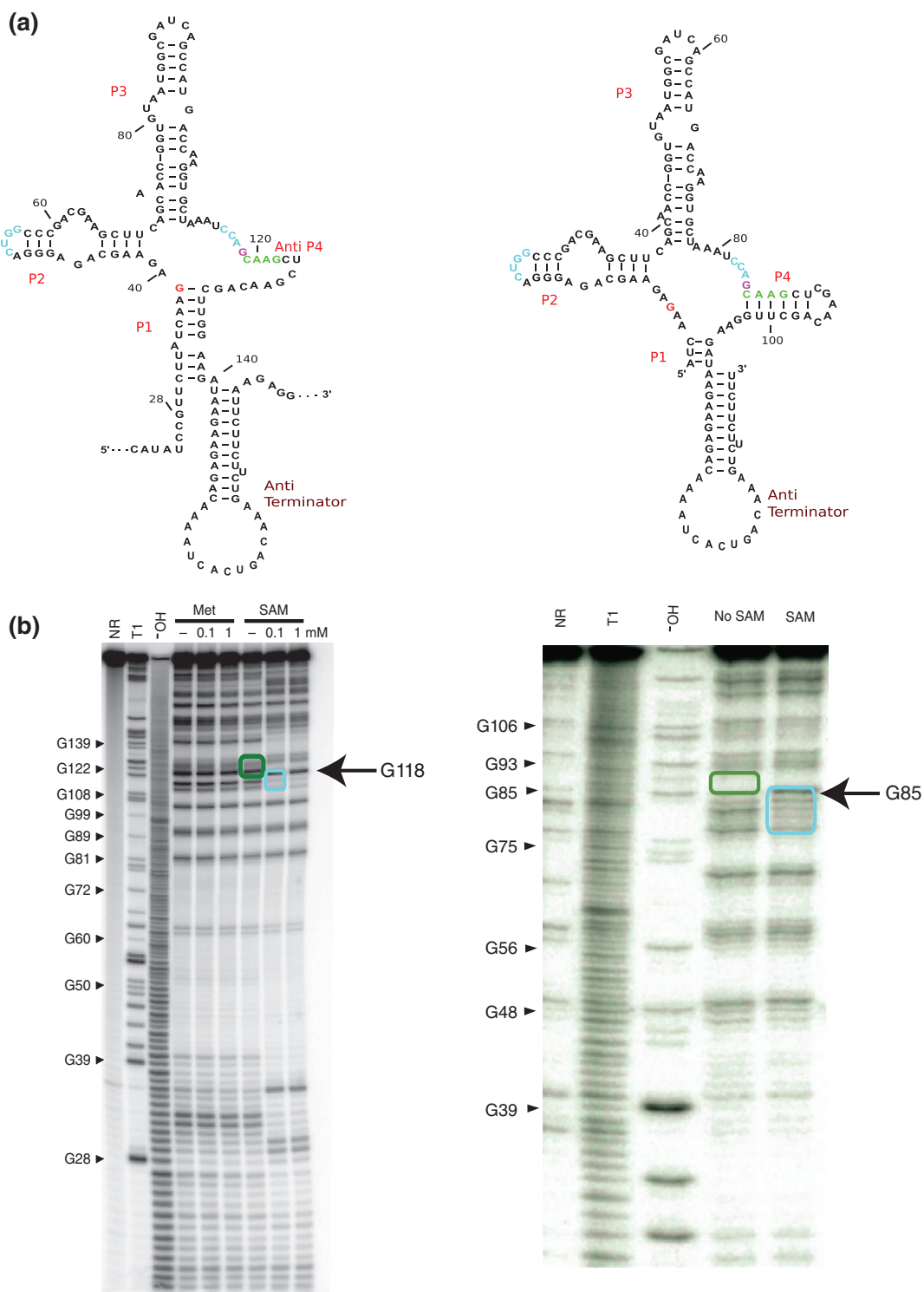


**FIGURE 4** | Alternative folds of SAM-I riboswitch in the absence of ligand. (a) Putative secondary structure of *B. subtilis yitJ* SAM-I riboswitch 251 *yitJ* construct from Winkler et al. (left)<sup>49</sup> and 3P1\_10AT *yitJ* construct from Boyapati et al. (right)<sup>18</sup> with P1, P2, P3, P4, and anti P4 helices. Residues in cyan are involved in the formation of the pseudoknot. Residues indicated in green are required for formation of the Anti-P4 or the P4 helix in 251 *yitJ* and 3P1\_10AT *yitJ*, respectively. (b) In-line probing data of 251 *yitJ* (left) and 3P1\_10AT *yitJ* (right). The lanes NR, OH, and T1 indicate no reaction, alkaline hydrolysis, and RNase T1, respectively. Residues protected by pseudo knot interaction in the presence of SAM in both the constructs are indicated by a cyan box, green boxed bands correspond to green boxed residues in panel a. (b, left panel: Reprinted with permission from Ref 49. Copyright 2003 Macmillan)

bound-state conformation by ligand binding (Figure 5 top panel).

This putative strand migration mechanism is potentially present in other riboswitches. A binding-competent hybrid P1/antiterminator helix-forming has been detected in an NMR study of an adenine-sensing riboswitch at low temperatures.<sup>17</sup> Two secondary structures are detected with the ligand bound, one of which is also present in the absence of ligand. The secondary structure of this binding-competent non-aptamer-containing conformer contains base pairings in common with both the terminator helix and the competing aptamer P1 helix. The authors propose that at low temperature, where folding kinetics is slow, the formation of the binding-competent conformer facilitates a timely transition to the ligand-bound aptamer state, if sufficient ligand is present.<sup>20</sup> This mechanism deviates from early assumptions, in that the expression platform

must be partially transcribed before the binding-competent state is present, in agreement with more recent cotranscriptional folding simulations.<sup>11,13</sup>

A strand migration mechanism for ligand-induced folding requires a nucleation of a minimal helix in order to allow ligand binding. Partial antiterminator formation may stabilize this nucleation. Prior to transcription of the expression platform, a short P1 nucleation will be unstable and may dissociate before the ligand can bind. Following partial synthesis of the expression platform, the ligand could accelerate P1 helix propagation by stabilizing transition states containing a hybrid P1/AT helix (or P1/T helix for a positively regulated riboswitch). By reducing the free energy barrier between proto-antiterminator forming conformers, which contain no P1 helix base pairs, and the partially nucleated transition state(s), the ligand would catalyze the rapid conversion to a P1

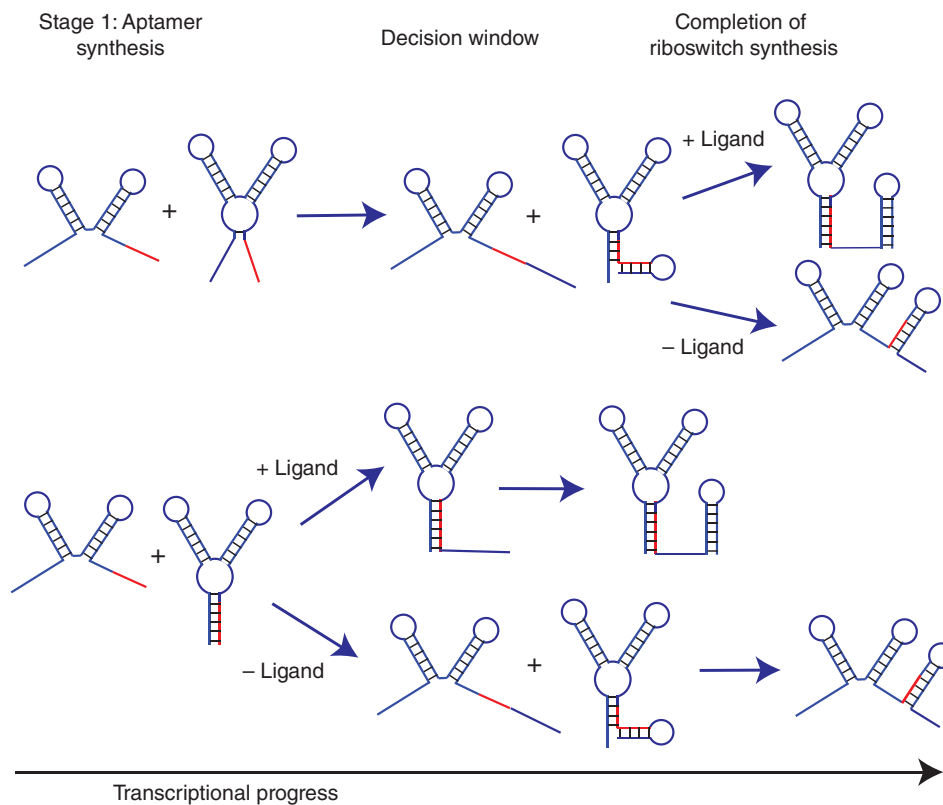


**FIGURE 5** | Schematic models for kinetic control of riboswitch folding and gene expression outcome during transcription, illustrating the role of multiple competing conformations. Top panel, the P1 helix does not form and nucleate sufficient P1 base pairs for ligand binding until other binding-competent intermediates form during the 'decision window', when the expression platform is being transcribed. The bottom panel illustrates a modified picture of kinetic trapping. The aptamer folds as it is transcribed—the ligand binds and fixes the aptamer fold, blocking the nucleation of the competing helix or blocking its formation via branch migration. Depending on whether the riboswitch is a positive or negative regulator, an additional terminator helix may form further downstream in the absence of the competing 'antiterminator' helix. These two models should not be viewed as mutually exclusive. In fact, varying combinations of the two are likely in different riboswitches, and even when a single riboswitch is transcribed in different cellular environments.

helix-facilitating formation of a downstream terminator helix (or antiterminator for a positively regulated system).

On the other hand, the ligand may not need to bind to the hybrid state to cause P1 helix formation, if the nucleated base pairs are stable enough to allow ligand binding. In that case, simulations for the SAM-I riboswitch<sup>19</sup> indicate that the bound ligand will promote completion of the P1 helix, blocking extension of the antiterminator helix via branch migration, until the terminator helix-forming region is transcribed (Figure 5, bottom panel). Interestingly, a construct carrying a full length P1 helix within the context of an antiterminator helix in a nonoverlapping region is still a weaker binder to SAM than the truncated aptamer.<sup>18</sup>

### Visualization of the Switching Trajectory Using the FEL

The last two systems present examples of transcriptional riboswitch conformers that are binding competent but that logically should function as predicted for the competing fold.<sup>17,18</sup> The fact that binding is reduced as compared with the aptamer fold means that ligand binding can drive the equilibrium rapidly toward the aptamer. Branch migration, involving small steps with small energy barriers, is predicted to be the fastest pathway for interconversion between alternative helical base pairing configurations.<sup>68,74</sup>

Figure 6 illustrates schematically this structure-interconversion mechanism from the perspective of the FEL. In the absence of ligand (Figure 6(a)), each possible RNA conformation has an associated free energy for the system of RNA plus solvent. The multi-dimensional conformational space represents overall configurations of the system. The distance between two states is related to the number of steps (changes in bond rotation, position of solvent molecule or ion, etc.) required to convert from one state to the other. In the presence of ligand, the free energy must now include that for the RNA plus ligand plus solvent. If we represent this new free energy plotted against the RNA conformation only (Figure 6, (b) and (c)), the free energy for those conformers that have any favorable binding free energy is now lowered as compared with those that do not, by an amount proportional to the binding free energy. In an idealized ‘conformational capture’ model (Figure 6(b)), only one state would be thus affected. If there are other binding-competent states, or a binding-competent region of conformational space, there will be more profound changes in the FEL (Figure 6(c)). This perturbed FEL will open new pathways for RNA folding and thus modify the kinetics of folding.

The functional consequences of ligand binding to an intermediate state have been explored by Fuertig et al.<sup>20</sup> for the special case of a ‘three state system’. They predicted switching efficiency—the percentage of total riboswitch RNA that undergoes a conformational transition toward the holo state upon a given increase in ligand concentration—as a function of temperature.<sup>20</sup> Their calculations illustrate the potential role of hitherto ignored heterogeneous conformers, previously dismissed as ‘misfolded’, in tuning riboswitch function to meet the dynamic requirements of the cell.

Evidence that residues even further downstream play a role in the regulatory activity of the adenine-responsive riboswitch comes from the P1 helix length dependence of transcription activation by the ligand.<sup>75</sup> A minimal P1 helix (three base pairs) was sufficient to trigger the formation of the terminator helix, but mutations further downstream, not directly involved in strand switching, were also found to affect the outcome. Terminator segments contain slippery sequences, leading to further possibilities for strand migration and base pairing slippage.

### Mechanisms for Fine Tuning of Riboswitch Function

It cannot be overemphasized that riboswitch mechanisms will not only vary with cellular conditions. They also vary between riboswitches—even within the same family and species. A powerful aspect of the riboswitch mechanism is that the versatile properties of RNA can be exploited to tune the response of a diverse set of genes, coding for diverse metabolic functions, to diverse metabolic conditions. A study of 11 SAM-I riboswitches in *B. subtilis* found a range of response thresholds to the ligand.<sup>26</sup> As the riboswitches sit upstream of genes involved in a number of stages within related metabolic cycles, the full network of riboswitch-regulated genes require a mechanism for fine tuning of the cell’s metabolism to fluctuating environmental conditions, as sensed by the cellular levels of the cognate and analog ligands.

Dynamic modeling and biophysical analysis of diverse SAM-I riboswitch sequences present possible mechanisms to explain these variations. A highly conserved G residue in J12, which makes a critical contact with the ligand, is predicted to form base pairs with an exceptional number of partner residues in the absence of SAM<sup>13</sup> (Figure 7, left). The ligand contact therefore blocks a range of potential alternative folds and acts as a chaperone to funnel the folding pathway toward the aptamer configuration (Figure 7, right). Considering the P1 helix-regulated mechanism, it is easy to see

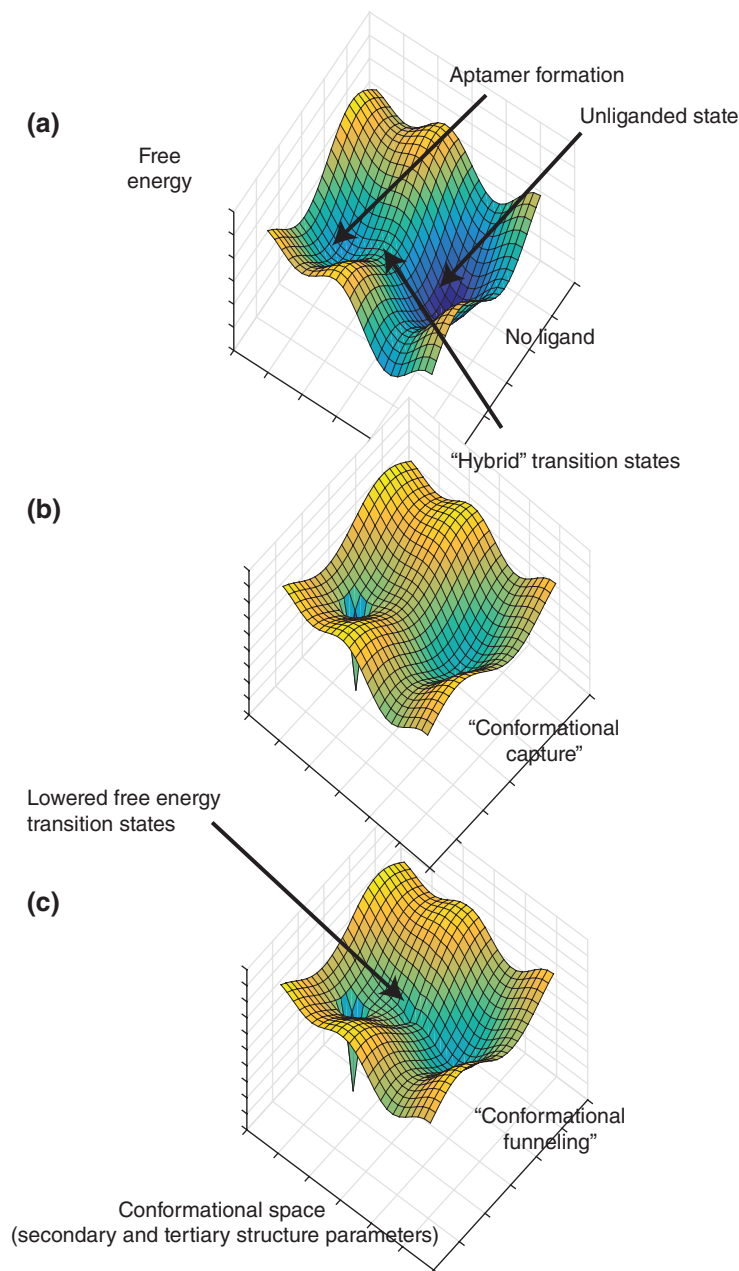


**FIGURE 6** | Schematic illustration of models for how ligand binding may perturb riboswitch folding thermodynamically or kinetically, as they would appear on the free energy landscape (FEL). (a) In the absence of ligand, the FEL represents the free energy linked to each possible secondary and tertiary structure fold of the RNA. The horizontal axes represent the multidimensional RNA conformational space. (b) In the presence of ligand, the FEL represents the free energy of the system of RNA + ligand. According to the ‘conformational capture’ model, the free energy of a single RNA conformation is bound by the ligand, leading to a dip in free energy corresponding to the binding affinity, while the relative free energy of other conformers is unaffected. (c) If the ligand also binds, with reduced affinity, to a subset of conformers (called ‘binding competent’), then the corresponding regions of conformational space also display a more modest dip in free energy. If the binding-competent region includes ‘transition states’ in the aptamer folding pathway, then the aptamer formation will be facilitated kinetically as well as thermodynamically.

how this ‘hot-spot’ for riboswitch conformational flexibility acts as a control point for ligand-mediated RNA folding.

Interestingly, base pairing probability calculations for a series of natural SAM-I riboswitch sequences

show a correlation between the number of predicted partners for the equivalent G residue in J12<sup>13</sup> and the reported transcriptional activity in the absence of SAM for the study cited above.<sup>26</sup> While the significance of this correlation is not clear, it is worth noting that

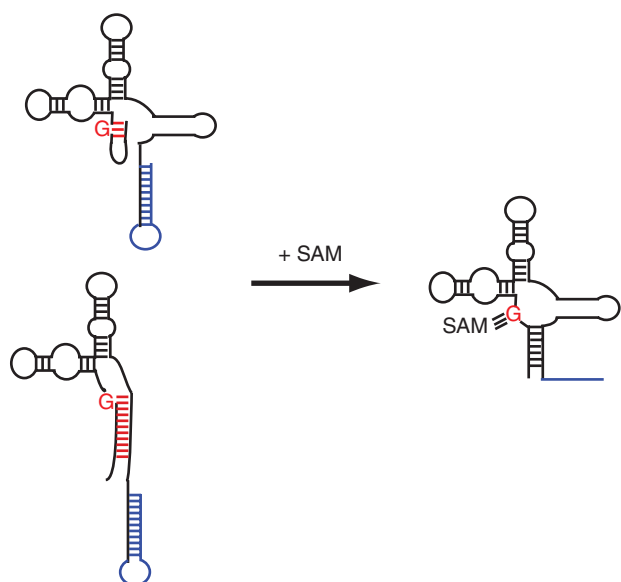


**FIGURE 7 |** Schematic illustration of ‘conformational collapse’ of the SAM-I riboswitch due to interaction of SAM with a hotspot G residue (highlighted in red) in junction J12. In the absence of SAM, the G residue in question is predicted to base pair with over 30 partners in alternative riboswitch conformers<sup>13</sup> (two of the lowest energy conformers are illustrated). SAM makes extensive contacts with the G residue, blocking alternative base pairings and alternative conformations. Residues 3’ of the aptamer are shown in blue. The schematic represents predicted riboswitch folding during the ‘sensing window’ when antiterminator, but not terminator transcription have been completed.

many riboswitch ligands contact G residues in the aptamer junction regions. Of all four canonical nucleotides, G residues are the most indiscriminate in their propensity to base pair with noncanonical partners.<sup>76</sup>

The strand switching mechanism requires a segment that ‘switches partners’ when ligand is present or absent. But each competing helix sometimes contains additional base pairs that do not participate in the switch. The extent of these nonoverlapping regions varies from one riboswitch to another and provides another potential tuning mechanism. An extended nonoverlapping region will facilitate nucleation of the corresponding helix in the presence or absence of ligand. In the *pbuE* adenine-responsive riboswitch extending the P1 helix to the point that it could compete with the closing base pair of a downstream helix (ordinarily not part of the competition region) disrupted the ligand sensitivity of the riboswitch.<sup>75</sup>

Synthetic transcriptional riboswitches designed to minimize the overlap between aptamer and expression platform achieve a regulatory response that is relatively independent of the expression platform.<sup>77</sup> Interestingly, activity in these riboswitches is far more sensitive to P1 helix length than in the case of the *pbuE* adenine-responsive riboswitch. This result may help to

explain how the variable nonoverlapping helical regions can tune riboswitch response to the specific requirements for regulation of downstream genes.

## IMPLICATIONS FOR DRUG DESIGN AND RIBOSWITCH ENGINEERING

A number of designed riboswitch aptamer ligands have been reported,<sup>78</sup> including a noncognate guanine riboswitch ligand with inhibitory activity against staph infection in a mammalian model.<sup>79</sup> Moreover, natural antibiotics such as roseoflavin have been shown to act against riboswitch targets. Nonetheless, drug design targeted at riboswitches remains a challenge. The participation of residues from the expression platform in the switching mechanism complicates strategies to inhibit riboswitch function that target the aptamer only.

The tetrahydrofolate (THF) riboswitch<sup>80</sup> illustrates the difficulty with targeting some riboswitches based only on ligand/aptamer affinity. As a depository for carbon moieties in cellular metabolism, THF coexists in the cell with a wide range of derivatives, many of which can bind the cognate riboswitch. The regulatory activity of the ligands is not correlated with binding affinities for the aptamer.<sup>81</sup>

This variable functional response to binding by different ligands may enable the cell to respond appropriately to a cellular imbalance between reduced and oxidized forms of THF. Differential affinities for transient intermediate conformers could be one mechanism to achieve this variable response. MD simulations<sup>82</sup> and FRET measurements for the SAM-II riboswitch<sup>83</sup> (a translational riboswitch) suggest another model for achieving a variable response to ligand analogues. Simulations indicated that SAH binds in a complex with similar binding mode to the cognate ligand, SAM, yet the two studies suggest that a downstream SD is sequestered in the SAM-II complex but exposed in the complex with SAH.

The correlation between aptamer binding and regulatory response holds better for P1 helix-regulated riboswitches responding to purines, SAM, lysine, TPP, and FMN. It may therefore be feasible to design antibiotics based on their affinity for the aptamer in these cases. Nonetheless, it is worth considering the expression domain and conformational intermediates during the drug design process. The correlation between ligand binding and regulatory response may not hold for all inhibitors. More importantly, consideration of these more complex dynamics provides opportunities for novel drug design strategies that may produce inhibitors with favorable properties—for example—slower induction of resistance mutations. Targeting of

alternative, so-called ‘inactive’ conformations, is a well-established approach for protein-directed drug design.<sup>84</sup> The ribosome is a very dynamic target of a number of natural product antibiotics.<sup>85</sup>

The new insights into the switching mechanism also present increased opportunities for riboswitch engineering. Mechanisms involving strand migration, long-range tertiary interactions, and transient intermediates are being exploited by natural riboswitches, in concert with pausing and careful calibration of folding and binding kinetics. These factors are finely balanced to tune function to different cellular conditions and to satisfy different cellular requirements. This strategy has some attractions for synthetic biology, if a mechanistic model can rationally predict ligand affinity and riboswitch response.

## CONCLUSION

From the literature cited in this review, we may propose a high-level description of how the riboswitch ligand perturbs RNA folding, at least for some riboswitches. The ligand modifies the FEL of a riboswitch in a concentration dependent manner. Not only the relative heights of the on and off folds, but energy barriers between intermediate states are also perturbed. Therefore, the presence of ligand affects not only the equilibrium between two dominant, alternative folds, but also determines when and how fast one structure converts to the other.

The role of strand migration in ligand-induced conformational switching presents a major challenge to experimental investigators. Short of observing all processes: transcription, binding, folding, pausing, in a single real-time experiment, measurements of ligand effects on riboswitch folding kinetics may give some direct and indirect insights into this aspect of the process. Single-molecule methods may illuminate the distinction between folding intermediates and ‘misfolded’ structures. The mechanism(s) responsible for pausing and termination during transcription, and the coupling of these outcomes to transcript folding are poorly understood. Further studies using single-molecule methods,<sup>86</sup> as well as structural studies of transcription complexes,<sup>87</sup> among other methods, can help address pausing mechanisms. Consideration of rate constants for ligand binding and RNA folding, the presence of conformational intermediates and

differential binding rates/affinities may appear to introduce arduous complications to our analysis of riboswitches. Nonetheless precedents for utilizing statistical mechanics and stochastic analysis to model dynamic processes in gene expression go back some decades (see additional reading).

That long-range folding can be so sensitive to a single functional group in a distal binding ligand is testimony to the remarkable functional versatility of RNA molecules. Traditional descriptions of the Central Dogma suggest that unique 3D folding of proteins facilitates unique functions, whereas Watson–Crick base pairing in nucleic acids is the ideal mechanism for storing, transmitting, and decoding information. Riboswitches stand that picture on its head. A unique 3D pattern of contacts is used to decode information regarding the cell’s state. Watson–Crick pairing in these systems facilitates structural polymorphism in response to this information-in effect acting as a mechanism for signal transduction. We should understand from riboswitches that while proteins are better suited for certain functions such as catalysis, RNA is ideally suited to tasks that require the cell to detect and respond ‘on the fly’ to environmental conditions.

These considerations should influence how we think about applications of riboswitch engineering. It is worth noting that the ability of aptamers, which are obtained via *in vitro* synthesis and selection,<sup>1</sup> to act as specific and selective chelators to a wide range of ligands has had information-related applications, such as imaging<sup>88</sup> and diagnosis.<sup>89</sup> Coupling this ability to the genetic decision-making ability of the expression platform has already resulted in a repertoire of devices that can control gene expression by interfering at various stages of mRNA synthesis and stability,<sup>4</sup> acting *in vitro* and *in vivo*, in prokaryotes and eukaryotes.<sup>90</sup> Riboswitches appear therefore to be readily amenable to rational design. It is important to note, however, that many of these designed riboswitches do not conform to the P1 helix-regulated pattern that is found in so many common riboswitches.

Drug design targeting riboswitches, perhaps not surprisingly, is a more challenging task. Nonetheless, a more sophisticated understanding of riboswitch function opens the way for new strategies as well as a means for interpreting previously unpredictable results from traditional approaches.

## FURTHER READING

Ken Dill SB. *Molecular Driving Forces: Statistical Thermodynamics in Biology, Chemistry, Physics, and Nanoscience*. 2nd ed. Garland Science, New York, London; 2010.



Wyman J. Regulation in macromolecules as illustrated by haemoglobin. *Q Rev Biophys* 1968, 1:35–80. doi:10.1017/S0033583500000457.

McGhee JD, von Hippel PH. Theoretical aspects of DNA-protein interactions: co-operative and non-co-operative binding of large ligands to a one-dimensional homogeneous lattice. *J Mol Biol* 1974, 86:469–489. doi:10.1016/0022-2836(74)90031-X.

Henkin TM, Yanofsky C. Regulation by transcription attenuation in bacteria: how RNA provides instructions for transcription termination/antitermination decisions. *Bioessays* 2002, 24:700–707. doi:10.1002/bies.10125.

Henkin TM. Editor—riboswitches. *Biochim Biophys Acta* 2014, 1839:899.

Draper DE. Folding of RNA tertiary structure: linkages between backbone phosphates, ions, and water. *Biopolymers* 2013, 99. doi:10.1002/bip.22249.

Cruz JA, Westhof E. The dynamic landscapes of RNA architecture. *Cell* 2009, 136:604–609.

## REFERENCES

1. Tuerk C, Gold L. Systematic evolution of ligands by exponential enrichment: RNA ligands to bacteriophage T4 DNA polymerase. *Science* 1990, 249:505–510.
2. Topp S, Gallivan JP. Emerging applications of riboswitches in chemical biology. *ACS Chem Biol* 2010, 5:139–148.
3. Wittmann A, Suess B. Engineered riboswitches: expanding researchers' toolbox with synthetic RNA regulators. *FEBS Lett* 2012, 586:2076–2083.
4. Weigand JE, Suess B. Tetracycline aptamer-controlled regulation of pre-mRNA splicing in yeast. *Nucleic Acids Res* 2007, 35:4179–4185.
5. Deigan KE, Ferré-D'Amaré AR. Riboswitches: discovery of drugs that target bacterial gene-regulatory RNAs. *Acc Chem Res* 2011, 44:1329–1338.
6. Blount KF, Breaker RR. Riboswitches as antibacterial drug targets. *Nat Biotechnol* 2006, 24:1558–1564.
7. Warner KD, Homan P, Weeks KM, Smith AG, Abell C, Ferré-D'Amaré AR. Validating fragment-based drug discovery for biological RNAs: lead fragments bind and remodel the TPP riboswitch specifically. *Chem Biol* 2014, 21:591–595.
8. Henkin TM. Riboswitch RNAs: using RNA to sense cellular metabolism. *Genes Dev* 2009, 22:3383–3390.
9. Batey RT. Structure and mechanism of purine-binding riboswitches. *Q Rev Biophys* 2012, 45:345–381.
10. Serganov A, Nudler E. A decade of riboswitches. *Cell* 2013, 152:17–24.
11. Quarta G, Sin K, Schlick T. Dynamic energy landscapes of riboswitches help interpret conformational rearrangements and function. *PLoS Comput Biol* 2012, 8: e1002368.
12. Quarta G, Kim N, Izzo JA, Schlick T. Analysis of riboswitch structure and function by an energy landscape framework. *J Mol Biol* 2009, 393:993–1003.
13. Huang W, Kim J, Jha S, Aboul-ela F. Conformational heterogeneity of the SAM-I riboswitch transcriptional ON State: a chaperone-like role for S-adenosylmethionine. *J Mol Biol* 2012, 418:331–349.
14. Wickiser JK, Winkler WC, Breaker RR, Crothers DM. The speed of RNA transcription and metabolite binding kinetics operate an FMN riboswitch. *Mol Cell* 2005, 18:49–60.
15. Wickiser JK, Cheah MT, Breaker RR, Crothers DM. The kinetics of ligand binding by an adenine-sensing riboswitch. *Biochemistry* 2005, 44:13404–13414.
16. Garst AD, Porter EB, Batey RT. Insights into the regulatory landscape of the lysine riboswitch. *J Mol Biol* 2012, 423:17–33.
17. Reining A, Nozinovic S, Schlepckow K, Buhr F, Furtig B, Schwalbe H. Three-state mechanism couples ligand and temperature sensing in riboswitches. *Nature* 2013, 499:355–359.
18. Boyapati VK, Huang W, Spedale J, Aboul-ela F. Basis for ligand discrimination between ON and OFF state riboswitch conformations: the case of the SAM-I riboswitch. *RNA* 2012, 18:1230–1243.
19. Huang W, Kim J, Jha S, Aboul-ela F. The impact of a ligand binding on strand migration in the SAM-I riboswitch. *PLoS Comput Biol* 2013, 9:e1003069.
20. Fuertig B, Nozinovic S, Reining A, Schwalbe H. Multiple conformational states of riboswitches fine-tune gene regulation. *Curr Opin Struct Biol* 2015, 30:112–124.
21. Barrick J, Breaker R. The distributions, mechanisms, and structures of metabolite-binding riboswitches. *Genome Biol* 2007, 8:R239.
22. Nawrocki EP, Burge SW, Bateman A, Daub J, Eberhardt RY, Eddy SR, Floden EW, Gardner PP, Jones TA, Tate J, et al. Rfam 12.0: updates to the RNA families database. *Nucleic Acids Res* 2015, 43:D130–D137.
23. Smith AM, Fuchs RT, Grundy FJ, Henkin T. Riboswitch RNAs: regulation of gene expression by direct monitoring of a physiological signal. *RNA Biol* 2010, 7:104–110.

24. Serganov A, Patel DJ. Metabolite recognition principles and molecular mechanisms underlying riboswitch function. *Annu Rev Biophys* 2012, 41:343–370.
25. Vicens Q, Mondragón E, Batey RT. Molecular sensing by the aptamer domain of the FMN riboswitch: a general model for ligand binding by conformational selection. *Nucleic Acids Res* 2011, 39:8586–8598.
26. Tomsic J, McDaniel BA, Grundy FJ, Henkin TM. Natural variability in S-Adenosylmethionine (SAM)-dependent riboswitches: S-Box elements in *Bacillus subtilis* exhibit differential sensitivity to SAM *in vivo* and *in vitro*. *J Bacteriol* 2008, 190:823–833.
27. DebRoy S, Gebbie M, Ramesh A, Goodson JR, Cruz MR, van Hoof A, Winkler WC, Garsin DA. A riboswitch-containing sRNA controls gene expression by sequestration of a response regulator. *Science* 2014, 345:937–940.
28. Loh E, Dussurget O, Gripenland J, Vaitkevicius K, Tien-suu T, Mandin P, Repoila F, Buchrieser C, Cossart P, Johansson J. A trans-acting riboswitch controls expression of the virulence regulator PrfA in *Listeria monocytogenes*. *Cell* 2009, 139:770–779.
29. Dann CEI, Wakeman CA, Sieling CL, Baker SC, Irnov I, Winkler WC. Structure and mechanism of a metal-sensing regulatory RNA. *Cell* 2007, 130:878–892.
30. Mandal M, Lee M, Barrick JE, Weinberg Z, Emilsson GM, Ruzzo WL, Breaker RR. A glycine-dependent riboswitch that uses cooperative binding to control gene expression. *Science* 2004, 306:275–279.
31. Gao A, Serganov A. Structural insights into recognition of c-di-AMP by the ydaO riboswitch. *Nat Chem Biol* 2014, 10:787–792.
32. Nou XW, Kadner RJ. Adenosylcobalamin inhibits ribosome binding to btuB RNA. *Proc Natl Acad Sci USA* 2000, 97:7190–7195.
33. Eichhorn CD, Kang M, Feigon J. Structure and function of preQ1 riboswitches. *Biochim Biophys Acta* 2014, 1839:939–950.
34. Heppell B, Lafontaine DA. Folding of the SAM aptamer is determined by the formation of a K-turn-dependent pseudoknot. *Biochemistry* 2008, 47:1490–1499.
35. Winkler WC, Grundy FJ, Murphy BA, Henkin TM. The GA motif: an RNA element common to bacterial antitermination systems, rRNA, and eukaryotic RNAs. *RNA* 2001, 7:1165–1172.
36. Schroeder KT, Daldrop P, Lilley DM. RNA tertiary interactions in a riboswitch stabilize the structure of a kink turn. *Structure* 2011, 19:1233–1240.
37. Hennelly SP, Novikova IV, Sanbonmatsu KY. The expression platform and the aptamer: cooperativity between Mg<sup>2+</sup> and ligand in the SAM-I riboswitch. *Nucleic Acids Res* 2013, 41:1922–1935.
38. Appasamy SD, Ramlan EI, Firdaus-Raih M. Comparative sequence and structure analysis reveals the conservation and diversity of nucleotide positions and their associated tertiary interactions in the riboswitches. *PLoS One* 2013, 8:e73984.
39. Montange RK, Batey RT. Structure of the S-adenosylmethionine riboswitch regulatory mRNA element. *Nature* 2006, 441:1172–1175.
40. Lu C, Ding F, Chowdhury A, Pradhan V, Tomsic J, Holmes WM, Henkin TM, Ke A. SAM recognition and conformational switching mechanism in the *Bacillus subtilis* yitJ S Box/SAM-I riboswitch. *J Mol Biol* 2010, 404:803–818.
41. Gilbert SD, Rambo RP, Tyne DV, Batey RT. Structure of the SAM-II riboswitch bound to S-adenosylmethionine. *Nat Struct Mol Biol* 2008, 15:177–182.
42. Lu C, Smith AM, Fuchs RT, Ding F, Rajashankar K, Henkin TM, Ke A. Crystal structures of the SAM-III/SMK riboswitch reveal the SAM-dependent translation inhibition mechanism. *Nat Struct Mol Biol* 2008, 15:1076–1083.
43. Smith KD, Lipchock SV, Livingston AL, Shanahan CA, Strobel SA. Structural and biochemical determinants of ligand binding by the c-di-GMP riboswitch. *Biochemistry* 2010, 49:7351–7359.
44. Serganov A, Polonskaia A, Phan AT, Breaker RR, Patel DJ. Structural basis for gene regulation by a thiamine pyrophosphate-sensing riboswitch. *Nature* 2006, 441:1167–1171.
45. Edwards TE, Ferre-D'Amare AR. Crystal structures of the Thi-box riboswitch bound to thiamine pyrophosphate analogs reveal adaptive RNA-small molecule recognition. *Structure* 2006, 14:1459–1468.
46. Whitford PC, Schug A, Saunders J, Hennelly SP, Onuchic JN, Sanbonmatsu KY. Nonlocal helix formation is key to understanding S-Adenosylmethionine-1 riboswitch function. *Biophys J* 2009, 96:L7–L9.
47. Huang W, Kim J, Jha S, Aboul-ela F. A mechanism for S-adenosyl methionine assisted formation of a riboswitch conformation: a small molecule with a strong arm. *Nucleic Acids Res* 2009, 37:6528–6539.
48. Montange RK, Mondragón E, van Tyne D, Garst AD, Ceres P, Batey RT. Discrimination between closely related cellular metabolites by the SAM-I riboswitch. *J Mol Biol* 2010, 396:761–772.
49. Winkler WC, Nahvi A, Sudarsan N, Barrick JE, Breaker RR. An mRNA structure that controls gene expression by binding S-adenosylmethionine. *Nat Struct Biol* 2003, 10:701–707.
50. Heppell B, Blouin S, Dussault A-M, Mulhbach J, Ennifar E, Penedo JC, Lafontaine DA. Molecular insights into the ligand-controlled organization of the SAM-I riboswitch. *Nat Chem Biol* 2011, 7:384–392.
51. Priyakumar UD, MacKerell AD Jr. Role of the adenine ligand on the stabilization of the secondary and tertiary interactions in the adenine riboswitch. *J Mol Biol* 2010, 396:1422–1438.

52. Greenleaf WJ, Frieda KL, Foster DAN, Woodside MT, Block SM. Direct observation of hierarchical folding in single riboswitch aptamers. *Science* 2008, 319:630–633.
53. McGary K, Nudler E. RNA polymerase and the ribosome: the close relationship. *Curr Opin Microbiol* 2013, 16:112–117.
54. Perdrizet GA, Artsimovitch I, Furman R, Sosnick TR, Pan T. Transcriptional pausing coordinates folding of the aptamer domain and the expression platform of a riboswitch. *Proc Natl Acad Sci* 2012, 109:3323–3328.
55. Larson MH, Landick R, Block SM. Single-molecule studies of RNA polymerase: one singular sensation, every little step it takes. *Mol Cell* 2011, 41:249–262.
56. Baird NJ, Kulshina N, Ferré D'Amaré AR. Riboswitch function: flipping the switch or tuning the dimmer? *RNA Biol* 2010, 7:328–332.
57. Lin J-C, Yoon J, Hyeon C, Thirumalai D. Using simulations and kinetic network models to reveal the dynamics and functions of riboswitches. *e-Print Archive, Quantitative Biology* 2014, arXiv:1410.0652v1:1–24.
58. Lee M-K, Gal M, Frydman L, Varani G. Real-time multidimensional NMR follows RNA folding with second resolution. *Proc Natl Acad Sci USA* 2010, 107:9192–9197.
59. Buck J, Wacker A, Warkentin E, Wöhnert J, Wirmer-Bartoschek J, Schwalbe H. Influence of ground-state structure and Mg<sup>2+</sup> binding on folding kinetics of the guanine-sensing riboswitch aptamer domain. *Nucleic Acids Res* 2011, 39:9768–9778.
60. Frieda KL, Block SM. Direct observation of cotranscriptional folding in an adenine riboswitch. *Science* 2012, 338:397–400.
61. Mayer G, Raddatz M-SL, Grunwald JD, Famulok M. RNA ligands that distinguish metabolite-induced conformations in the TPP riboswitch. *Angew Chem Int Ed* 2007, 46:557–560.
62. Lang K, Rieder R, Micura R. Ligand-induced folding of the thiM TPP riboswitch investigated by a structure-based fluorescence spectroscopic approach. *Nucleic Acids Res* 2007, 35:5370–5378.
63. Hennelly SP, Sanbonmatsu KY. Tertiary contacts control switching of the SAM-I riboswitch. *Nucleic Acids Res* 2011, 39:2416–2431.
64. Kim J, Huang W, Maddineni S, Aboul-ela F, Jha S. Energy landscape analysis for regulatory RNA finding using scalable distributed cyberinfrastructure. *Concurr Comput* 2011, 23:2292–2304.
65. Onuchic JN, Luthey-Schulten Z, Wolynes PG. Theory of protein folding: the energy landscape perspective. *Annu Rev Phys Chem* 1997, 48:545–600.
66. Sauerwine B, Widom M. Arrhenius lifetimes of RNA structures from free energy landscapes. *J Stat Phys* 2011, 142:1337–1352.
67. Ditzler MA, Rueda D, Mo J, Håkansson K, Walter NG. A rugged free energy landscape separates multiple functional RNA folds throughout denaturation. *Nucleic Acids Res* 2008, 36:7088–7099.
68. Gong S, Wang Y, Zhang W. Kinetic regulation mechanism of pbuE riboswitch. *J Chem Phys* 2015, 142:015103.
69. Lin J-C, Hyeon C, Thirumalai D. Sequence-dependent folding landscapes of adenine riboswitch aptamers. *Phys Chem Chem Phys* 2014, 16:6376–6382.
70. Anthony PC, Perez CF, García-García C, Block SM. Folding energy landscape of the thiamine pyrophosphate riboswitch aptamer. *Proc Natl Acad Sci* 2012, 109:1485–1489.
71. Nozinovic S, Reining A, Kim Y-B, Noeske J, Schlepckow K, Wöhnert J, Schwalbe H. The importance of helix P1 stability for structural pre-organization and ligand binding affinity of the adenine riboswitch aptamer domain. *RNA Biol* 2014, 11:655–666.
72. Neupane K, Ritchie DB, Yu H, Foster DAN, Wang F, Woodside MT. Transition path times for nucleic acid folding determined from energy-landscape analysis of single-molecule trajectories. *Phys Rev Lett* 2012, 109:068102.
73. Zhang W, Chen S-J. Exploring the complex folding kinetics of RNA hairpins: I. General folding kinetics analysis. *Biophys J* 2006, 90:765–777.
74. Zhao P, Zhang W-B, Chen S-J. Predicting secondary structural folding kinetics for nucleic acids. *Biophys J* 2010, 98:1617–1625.
75. Marcano-Velázquez JG, Batey RT. Structure-guided mutational analysis of gene regulation by the *Bacillus subtilis* pbuE adenine-responsive riboswitch in a cellular context. *J Biol Chem* 2014, 90:4464–4475.
76. Aboul-ela F, Koh D, Tinoco I Jr, Martin FH. Base-base mismatches. Thermodynamics of double helix formation for dCA3XA3G+dCT3YT3G(X, Y = A, C, G, T). *Nucleic Acids Res* 1985, 13:4811–4824.
77. Ceres P, Garst AD, Marcano-Velázquez JG, Batey RT. Modularity of select riboswitch expression platforms enables facile engineering of novel genetic regulatory devices. *ACS Synth Biol* 2013, 2:463–472.
78. Warner KD, Homan P, Weeks KM, Smith AG, Abell C, Ferré-D'Amaré AR. Validating fragment-based drug discovery for biological RNAs: lead fragments bind and remodel the TPP riboswitch specifically. *Chem Biol* 2014, 21:591–595.
79. Mulhbachter J, Brouillette E, Allard M, Fortier L-C, Malouin F, Lafontaine DA. Novel riboswitch ligand analogs as selective inhibitors of guanine-related metabolic pathways. *PLoS Pathog* 2010, 6:e1000865.
80. Ames TD, Rodionov DA, Weinberg Z, Breaker RR. A eubacterial riboswitch class that senses the coenzyme tetrahydrofolate. *Chem Biol* 2010, 17:681–685.
81. Trausch JJ, Batey RT. A disconnect between high-affinity binding and efficient regulation by antifolates and purines in the tetrahydrofolate riboswitch. *Chem Biol* 2014, 21:205–216.

82. Doshi U, Kelley JM, Hamelberg D. Atomic-level insights into metabolite recognition and specificity of the SAM-II riboswitch. *RNA* 2012, 18:300–307.
83. Haller A, Rieder U, Aigner M, Blanchard SC, Micura R. Conformational capture of the SAM-II riboswitch. *Nat Chem Biol* 2011, 7:393–400.
84. Noble MEM, Endicott JA, Johnson LN. Protein kinase inhibitors: insights into drug design from structure. *Science* 2004, 303:1800–1805.
85. Ogle JL, Murphy FV, Tarry MJ, Ramakrishnan V. Selection of tRNA by the ribosome requires a transition from an open to a closed form. *Cell* 2002, 111:721–732.
86. Maoiléidigh DO, Tadigotla VR, Nudler E, Ruckenstein AE. A unified model of transcription elongation: what have we learned from single-molecule experiments? *Biophys J* 2011, 100:1157–1166.
87. Epshtein V, Cardinale CJ, Ruckenstein AE, Borukhov S, Nudler E. An allosteric path to transcription termination. *Mol Cell* 2007, 28:991–1001.
88. Wang AZ, Farokhzad OC. Current progress of aptamer-based molecular imaging. *J Nucl Med* 2014, 55:353–356.
89. Reinemann C, Strehlitz B. Aptamer-modified nanoparticles and their use in cancer diagnostics and treatment. *Swiss Med Wkly* 2014, 144:w13908.
90. Wittmann A, Suess B. Engineered riboswitches: expanding researchers' toolbox with synthetic RNA regulators. *FEBS Lett* 2012, 586:2076–2083.